International Journal of Mass Spectrometry 313 (2012) 15–20

Contents lists available at SciVerse ScienceDirect

International Journal of Mass Spectrometry

journal homepage: www.elsevier.com/locate/ijms

Metastable fragmentation of a thymidine-nucleotide and its components

Ilko Bald*,[1], Helga D. Flosadóttir, Benedikt Ómarsson, Oddur Ingólfsson*

University of Iceland, Science Institute, Faculty of Science, Department of Chemistry, 107 Reykjavik, Iceland

ARTICLE INFO

Article history:
Received 25 October 2011
Received in revised form 2 December 2011
Accepted 13 December 2011
Available online 30 December 2011

Keywords:
Matrix-assisted laser desorption/ionization (MALDI)
Negative ions
DNA radiation damage

ABSTRACT

In aqueous biological environment DNA is typically deprotonated. The metastable deprotonated DNA nucleobases are important reaction intermediates in low-energy electron induced damage to DNA. By comparing the metastable decay of small deprotonated DNA building blocks (thymine, thymidine, D-ribose, D-ribose 5-monophosphate) with the metastable decay of thymidine 5′-monophosphate and the hexameric oligonucleotide dT_6 we show that the most intense fragmentation pathways of the individual components are inherited to their *next larger* compositions of one step further in complexity, i.e., from thymine and ribose to thymidine, from thymidine and 2-deoxyribose 5-monophosphate to thymidine 5′-monophosphate, and from thymidine 5′-monophosphate to thymine oligonucleotides. However, fragmentation channels that are dominant in the smaller, principle building blocks such as D-ribose and thymidine do not necessarily prevail beyond their composition, i.e., in thymidine 5′-monophosphate and thymine oligonucleotides. The comparison of the metastable decay mass spectra of molecules of increasing complexity reveals detailed fragmentation mechanisms and shows that the individual fragmentation pathways are determined by the initial deprotonation sites.

1. Introduction

The damage of DNA and its components by ionizing radiation is to a large extent ascribed to fragmentation induced by secondary low-energy electrons (<10 eV) [1,2]. Numerous studies were devoted to the question of how low-energy electrons induce the most severe types of DNA damage, namely DNA strand breaks, nucleobase loss and nucleobase lesions [3]. The pivotal reaction mechanism is dissociative electron attachment (DEA) [4] and consequently a number of detailed DEA studies with the single DNA building blocks in the gas phase have been conducted [3]. These include studies on the individual nucleobases [5], the sugar moiety [6,7] and the phosphate group [8,9]. The investigation of the individual building blocks reveals detailed fragmentation mechanisms, but a complete picture of the relevant fragmentation processes can only be gained when increasingly complex systems are investigated. Gas phase DEA studies are hampered by the challenge to transport the fragile neutral biomolecules intact into the gas phase [8]. Therefore, the largest compounds investigated so far in the gas phase with respect to DEA are the nucleoside thymidine [10] and the RNA backbone model compound ribose 5-monophosphate [8].

The initial step in the DEA process is the formation of a transient negative ion with the extra electron occupying a formerly empty molecular orbital. The negative ion state might be repulsive and can dissociate within a very short time scale (tens of fs) [4]. The main fragmentation pathway of transient DNA nucleobase anions (and in general most organic TNIs) proceeds through the abstraction of a hydrogen atom [3,5,11]. The dehydrogenated anion was shown to be an important metastable precursor for most other fragmentation products observed in DEA to the nucleobase thymine [12]. The dehydrogenated anion is equivalent to the deprotonated molecule that can be easily generated by matrix-assisted laser desorption and ionization (MALDI) [13]. In the present study we compare the metastable decay of deprotonated DNA building blocks at different levels of complexity. We start by considering the isolated nucleobase thymine and the sugar D-ribose, and then proceed over the nucleoside thymidine and the sugar phosphates to the nucleotide thymidine 5′-phosphate and the deprotonated hexameric oligonucleotide dT_6. In this study, the deprotonated DNA building blocks are generated by MALDI and analyzed by time-of-flight mass spectrometry. Deprotonation occurs through proton exchange between the sample molecule and the matrix. For molecules which have more than one available site for deprotonation, several different ions are formed, according to the gas phase acidity (GPA) of the removed protons. The time frame of the metastable decay in these experiments is 5–20 μs. The mass spectra obtained from small molecules yield detailed information

* Corresponding authors. Tel.: +4587155861 (I. Bald), +354 5254313 (O. Ingólfsson).
E-mail addresses: ibald@zedat.fu-berlin.de, ibald@inano.au.dk (I. Bald), odduring@hi.is (O. Ingólfsson).
[1] Present address: Interdisciplinary Nanoscience Center (iNANO), Department of Physics and Astronomy, University of Aarhus, Denmark.

1387-3806/$ – see front matter © 2011 Elsevier B.V. All rights reserved.
doi:10.1016/j.ijms.2011.12.007

Table 1
Summary of fragment anions observed after metastable decay of deprotonated thymine, ribose, thymidine, 2-deoxyribose 5-monophosphate, ribose 5-monophosphate, and thymidine 5′-monophosphate. The fragmentation types are indicated in the first column and can be classified as nucleobase ring cleavage, sugar cross-ring cleavage, glycosidic bond cleavage and phosphate ester cleavage.

Deprotonated precursor Bond rupture	*m/z*	Negative ion fragment	Neutral fragments
Thymine	125	$C_5H_5N_2O_2^-$	
Nucleobase ring cleavage	42	NCO^-	C_4H_5NO
D-ribose	149	$C_5H_9O_5^-$	
Water loss	131	$C_5H_7O_4^-$	H_2O
Sugar cross-ring cleavage	119	$C_4H_7O_4^-$	CH_2O
Sugar cross-ring cleavage	100	$C_4H_4O_3^-$	$CH_2O + H_2O + H$
Sugar cross-ring cleavage	89	$C_3H_5O_3^-$	$C_2H_4O_2$
Sugar cross-ring cleavage	71	$C_3H_3O_2^-$	$C_2H_4O_2 + H_2O$
Thymidine	241	$[dT - H]^-$	
Sugar cross-ring cleavage	151	$[(T - H) + C_2H_2]^-$	$C_3H_6O_3$
Glycosidic cleavage	125	$[T - H]^-$	$C_5H_8O_3$
Nucleobase ring cleavage	42	NCO^-	$C_5H_8O_3C_4H_5NO$
2-Deoxyribose 5-monophosphate	213	$HPO_4C_5H_9O_3^-$	
Sugar cross-ring cleavage	169	$HPO_4C_3H_5O_2^-$	C_2H_4O
Sugar cross-ring cleavage	152	$HPO_4C_3H_4O^-$	$C_2H_5O_2$
Sugar cross-ring cleavage	139	$HPO_4C_2H_3O^-$	$C_3H_6O_2$
PO—C	97	$H_2PO_4^-$	$C_5H_8O_3$
P—OC	79	PO_3^-	$C_5H_{10}O_4$
Ribose 5-monophosphate	229	$HPO_4C_5H_9O_4^-$	
Sugar cross-ring cleavage	169	$HPO_4C_3H_5O_2^-$	$C_2H_4O_2$
Sugar cross-ring cleavage	139	$HPO_4C_2H_3O^-$	$C_3H_6O_3$
PO—C	97	$H_2PO_4^-$	$C_5H_8O_4$
P—OC	79	PO_3^-	$C_5H_{10}O_5$
Thymidine 5′-monophosphate	321	$HPO_4C_5H_8O_2C_5H_5N_2O_2^-$	
Nucleobase ring cleavage	278	$[dT5P - HNCO]^-$	HNCO
Glycosidic cleavage	195	$[dT5P - T]^-$	T
Glycosidic cleavage	177	$[dT5P - T - H_2O]^-$	$T + H_2O$
Glycosidic cleavage	125	$[T - H]^-$	$HPO_4C_5H_8O_2$
PO—C	97	$H_2PO_4^-$	$C_5H_7O_2C_5H_5N_2O_2$
P—OC	79	PO_3^-	$C_5H_9O_3C_5H_5N_2O_2$

about fragmentation mechanisms and the study of larger molecules shows the relevance of individual reaction pathways in more complex systems. The anionic fragmentation products observed from all investigated molecules are summarized in Table 1.

2. Experimental methods

Metastable decay of the deprotonated molecules was measured in negative ion, post source decay (PSD) mode with a UV MALDI mass spectrometer (MALDI-MS) (Reflex IV, Bruker Daltonics, Bremen, Germany). The instrument and its operation has been described in detail elsewhere [14]. In brief, ions were generated during the MALDI process with an N_2-laser at 337 nm with a repetition rate of 7–10 Hz. The laser power was kept about 20% above the detection threshold for the corresponding ions. To average out sample inhomogeneity the laser spot was moved manually over the sample during acquisition. Negative ions were extracted in pulsed delayed extraction mode with a delay time of 200 ns and accelerated into a reflectron time-of-flight (ToF) mass spectrometer. The PSD spectra were recorded by gating selected parent ions into the field free linear region of the mass spectrometer. The mass gate was set at ±5 Da in all experiments. The total acceleration voltage into the field free linear region was 25 kV resulting in about 5–12 μs flight time depending on the ion mass. This was the time window within which we observed metastable decay. After the linear flight the ions were decelerated and reaccelerated with a grid-less reflectron and detected with a double micro-channel plate detector. The reflectron voltage was stepped down in 7–9 segments, depending on the sample, to assure for collection of all fragments. Individual segments are the sum of 500 shots, which were recorded by using the fragmentation analyses and structural ToF method FAST, within the instrumental control software FlexControl®. The alignment of individual segments and the mass calibration of the spectra was carried out with the FlexAnalysis® software also provided by the instrument manufacturer.

The sample molecules thymine, 1N-methylthymine, D-ribose, thymidine, ribose 5-monophosphate sodium salt, 2-deoxyribose 5-monophosphate and thymidine 5′-monophosphate were acquired from Sigma–Aldrich, Germany as high purity samples (>98%) and used without further purification. The thymine derivative 3N-methylthymine was prepared in-house from the respective nucleosides and bases. The preparation and purification protocol for 3N-methylthymine was performed as described by Breeger et al. [15], and the molecular structure was verified by H NMR. The hexameric oligonucleotide dT_6 was synthesized and purified in-house as described by Stano et al. [14]. After purification the sample was dried on a Thermosavant ISSI110 speedvac system and redissolved in 100 μL sterile purified water. The concentration was determined on a 500 times diluted sample by UV absorption at 260 nm. The sample was then separated into 10 μL portions and stored at −20 °C until use.

The MALDI-PSD samples were prepared by co-spotting 0.5 μL of a 1 mg/mL aqueous solution of the matrix bisbenzimide H33258; $C_{25}H_{24}N_6O{\cdot}3HCl$ (≥98%, Sigma–Aldrich, Germany) and 0.5 μL of a 10 mg/mL solution of the analyte (thymidine 5′-monophosphate and its components) in methanol on a stainless steel sample carrier. dT_6 (2 μL, 0.1 mmol/mL) was mixed with the matrix DHB (2 μL, 10 mg/mL) and acetonitrile (2 μL) and spotted in droplet size of 0.5 μL on a 400 μm AnchorChip® sample plate and let dry under atmospheric pressure and RT.

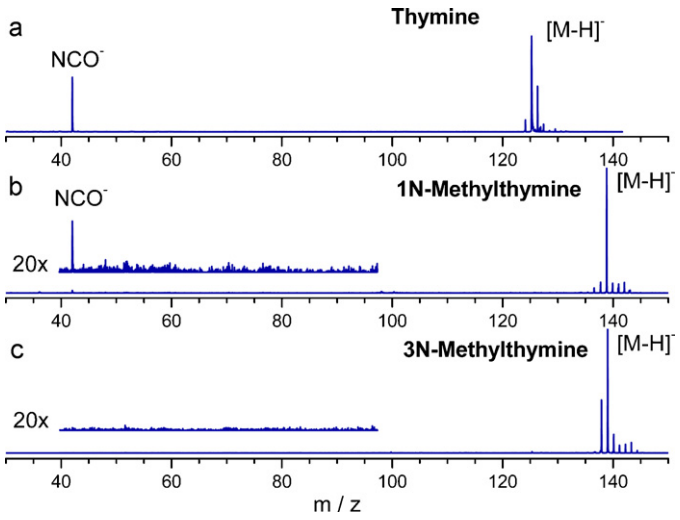

Fig. 1. Metastable decay mass spectrum of deprotonated T and the methylated derivatives 1NmeT and 3NmeT. The main observed product ion is NCO^-, which is not observed from 3NmeT indicating that deprotonation of T occurs from 3N.

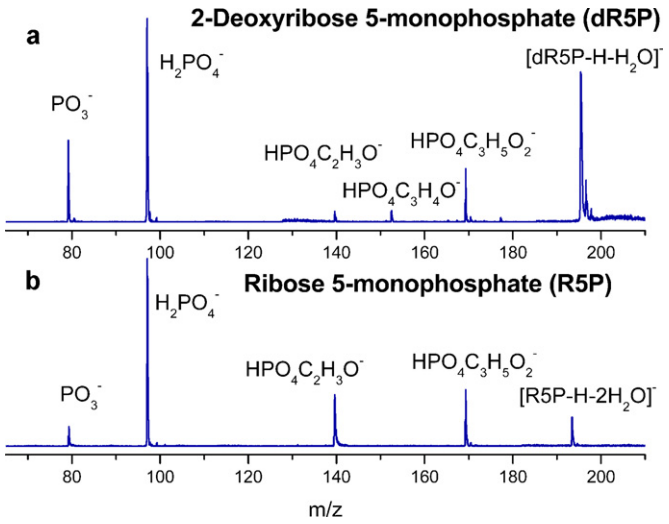

Fig. 3. Fragment mass spectra of sugarphosphates. Water loss, sugar cross ring cleavage and phosphate bond rupture are the main fragmentation pathways observed.

3. Results and discussion

The metastable decay mass spectrum of deprotonated thymine (T) obtained by MALDI is displayed in Fig. 1a showing the dominant fragment ion NCO^-.

The pyrimidine ring contains two nitrogen atoms (1N and 3N) that provide two possible origins of the NCO^- fragment. To reveal the site of NCO^- elimination we performed PSD measurements with the methylated thymine derivates 1N-methylthymine (1NmeT) and 3N-methylthymine (3NmeT), which are shown in Fig. 1b and c, respectively. Formation of the NCO^- fragment ion is observed in PSD of deprotonated 1NmeT, but not in 3NmeT. The methyl group in 3NmeT prevents deprotonation at 3N and thus further fragmentation. This indicates that the deprotonated precursor ion carries the negative charge at 3N, and hence it is likely that NCO^- exclusively contains 3N. Lamshabi et al. demonstrated with isotope labelled uracil that the formation of the NCO fragment from deprotonated uracil complexed with Cu^{2+} ions includes exclusively 3N and 2C [16]. DFT calculations suggested that the metal cation is located above the uracil plane forming a π-type complex that activates the 2C—1N bond, which results in selective NCO loss [16]. The present experiments indicate that activation by cation complexation is not required to induce a selective NCO^- formation from deprotonated thymine. From thymine deprotonated at 3N, NCO^- can be formed from 3N and 2C by reverse pericyclic cycloaddition as depicted in Fig. 5a. This process is thermodynamically driven by the high electron affinity of the NCO radical (3.609 eV)[17]. Due to the higher GPA of 1N—H compared to 3N—H (333 kcal/mol for 1N—H, 347 kcal/mol for 3N—H) [18] the corresponding anion with the charge located on N1 is more stable and ring cleavage does not proceed through deprotonation at 1N. This leads to a larger amount of anions deprotonated at 1N, but dissociation occurs only from 3N. In DNA the 1N proton of thymine is replaced by the N-glycosidic bond, but the 3N proton is still available. Consequently, deterioration of the thymine ring through deprotonation may also be an important reaction in larger systems.

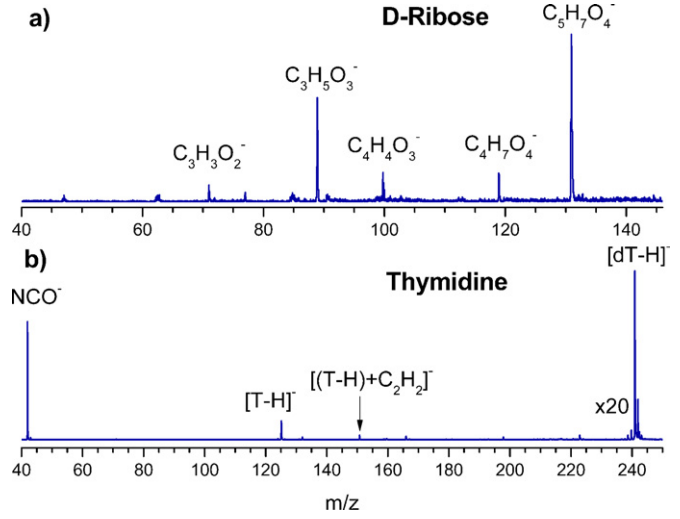

Fig. 2. Metastable decay mass spectra of deprotonated D-ribose and thymidine. Deprotonated D-ribose is subject to cross-ring cleavage, whereas deprotonated thymidine fragments by N-glycosidic bond cleavage and nucleobase ring cleavage (NCO^- formation). Spectra are adapted from [19,20].

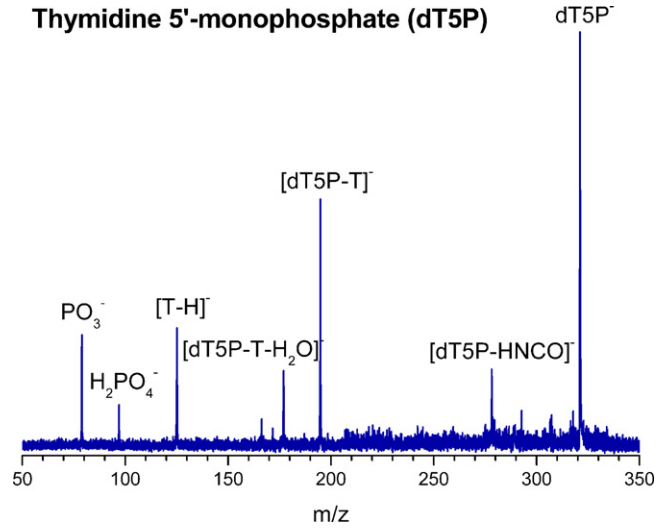

Fig. 4. Metastable decay mass spectrum of dT5P. Glycosidic bond cleavage and phosphate ion formation dominates and thymine ring rupture is observed.

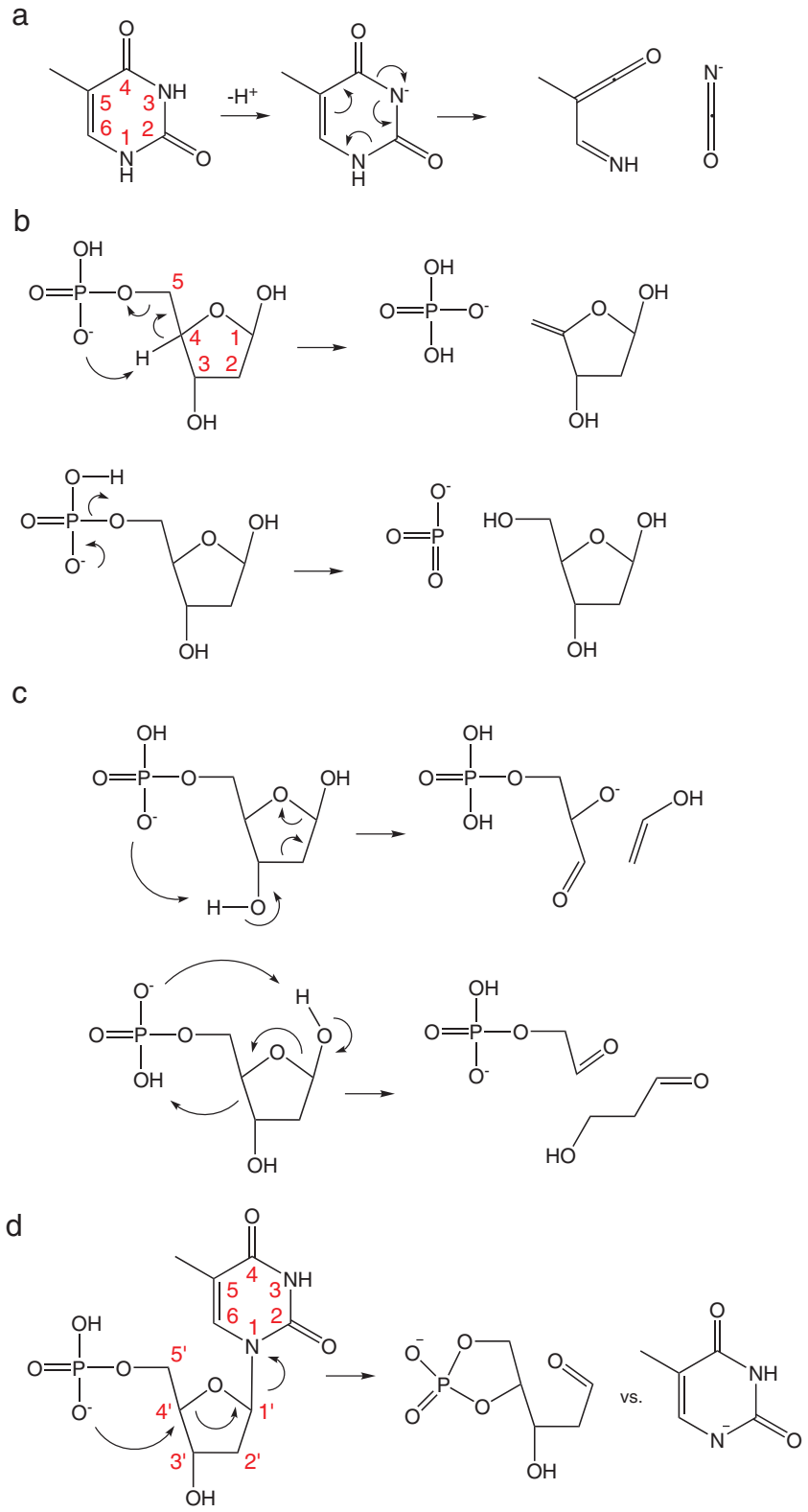

Fig. 5. Reaction scheme showing the most important fragmentation reactions of deprotonated DNA building blocks. (a) Cross-ring cleavage of deprotonated T resulting in NCO^- formation. This reaction is also observed in the larger molecules dT and dT5P. (b) Phosphate ion formation in dR5P, which is similarly observed in R5P and dT5P. (c) Sugar cross ring cleavage as observed in dR5P. d) Glycosidic bond cleavage in dT5P induced by nucleophilic attack of the phosphate group at 4′C.

Similar to the nucleobase thymine the sugar D-ribose is also subject to fragmentation upon deprotonation (Fig. 2a). As shown in previous studies fragmentation of deprotonated monosaccharides is characterized by elimination of different numbers of water molecules and cross-ring cleavage resulting in typical neutral fragments $C_nH_{2n}O_n$ [19]. By using different isotope labelled sugars it was shown that the cross ring cleavage proceeds site selectively where fragments are either formed exclusively through

fragmentation from the 5C end or exclusively from the 1C end. The most pronounced fragment from the deprotonated D-ribose, however, appears at *m/z* 89 and is formed through 4C and 5C loss as well as 1C and 2C loss from the sugar. With classical dynamics simulations it was demonstrated that the specific fragmentation pathways are determined by the position of deprotonation [21]. Deprotonation occurs most likely at the anomeric hydroxyl group (at 1C) or the hydroxyl group at 4C, which are the most acidic hydroxyl groups in D-ribose. The protons at other hydroxyl groups (at 2C and 3C) can however also be removed, but to a lesser extent. Isolated D-ribose adopts the pyranose form in the gas phase (six-membered ring). When it is bound via an N-glycosidic bond to a nucleobase (for instance in thymidine, see next paragraph) the furanose form is adopted, and neither the anomeric hydroxyl group nor the hydroxyl group at 4C is then available for deprotonation.

In the nucleoside thymidine (dT) deprotonation occurs most likely at the nucleobase, i.e., 3N. Consequently, in the PSD spectrum of deprotonated thymidine [20] (Fig. 2b) the most pronounced fragmentation pathway is a ring cleavage of the thymine subunit resulting in NCO^- formation in accordance to the results for bare thymine (Fig. 1). Furthermore, a cleavage of the glycosidic bond is observed resulting in the fragment anion $[T - H]^-$. In addition to the glycosidic bond cleavage and the thymine fragmentation also cross-ring cleavage of the sugar ring is observed, i.e., the elimination of neutral $C_3H_6O_3$. A detailed study on uridine derivatives protected at selected positions in conjunction with computational results indicates that glycosidic bond cleavage and sugar cross-ring cleavage of deprotonated thymidine is due to initial deprotonation of the 3′OH group of the sugar ring [20]. A deprotonation of 4′OH (as observed from D-ribose) is not possible in thymidine, since 4′OH is involved in the furanose ring formation. The comparatively high intensity of the NCO^-signal is ascribed to the high GPA of 3N—H compared to 3′OH.

Fig. 3 shows the metastable decay spectra of 2-deoxyribose 5-phosphate (dR5P, $HPO_4C_5H_9O_3$, *m/z* 213) and ribose-5-phosphate (R5P, $HPO_4C_5H_9O_4$, *m/z* 229). These components are principle building blocks of the DNA or RNA backbone, respectively. The dominating fragmentation channels are formation of the $H_2PO_4^-$ ion and, with lower intensity, formation of the PO_3^- ion. The GPA of H_3PO_4 is 319 kcal/mol [22] compared to 334 kcal/mol for α-D-glucose [23], which can be taken as a representative value for monosaccharides. Deprotonation of R5P and dR5P proceeds most likely from the phosphate group resulting in the formation of the phosphate ions $H_2PO_4^-$ and PO_3^- as shown in Fig. 5b. The negatively charged phosphate oxygen can form a hydrogen bond with 4C—H resulting in a six-membered transition state followed by elimination of $H_2PO_4^-$ (phosphate ester pyrolysis). Alternatively the PO_3^- ion can directly be abstracted by cleavage of the P—OC bond. More surprising is the observation of sugar cross-ring cleavage, i.e., the formation of $HPO_4C_3H_5O_2^-$ (*m/z* 169) and $HPO_4C_2H_3O^-$ (*m/z* 139). Since both these ions occur at the same *m/z* from dR5P and R5P the eliminated neutral counterparts must contain the anomeric centre (1C, see Fig. 5c) and its adjacent carbon atom. The same sugar cross-ring cleavage that results in *m/z* 139 in R5P was observed with high intensity in D-ribose at *m/z* 89[19], but with charge retention on the complementary fragment. The GPA of the involved fragments is not known, but it is likely that the phosphate containing fragment is more acidic than the fragments arising from the 1C site of the sugar (C_2H_4O and $C_3H_6O_2$ from dR5P). Consequently the charge remains on the phosphate containing fragment, leading to the observed fragment ion distribution. In addition to the phosphoester and cross-ring cleavage also water elimination is observed that might proceed by nucleophilic attack of the phosphate at 3C and formation of a six-membered cyclic phosphate involving 3C and 5C followed by elimination of water from 3OH.

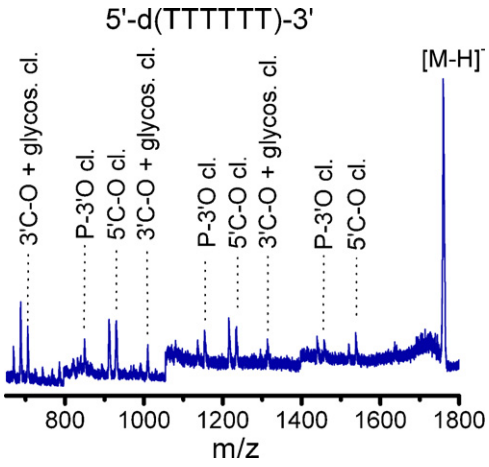

Fig. 6. Metastable decay spectrum of a deprotonated thymidine hexamer. The main fragmentation pathways are backbone breakage by dissociation of the 5′C—O, 3′C—O and P—3′O bonds. The double peaks are separated by 18 mass units indicating that additional water loss is operative. Apart from the phosphodiester bond cleavage also loss of the neutral nucleobases, i.e., glycosidic bond cleavage, is observed.

Fig. 4 shows the metastable decay spectrum of thymidine 5′-monophosphate (dT5P). Similar to the sugarphosphates the fragmentation of dT5P is governed by the phosphate group, but the presence of the nucleobase in dT5P leads to distinct differences. Glycosidic bond cleavage is the most dominant fragmentation of dT5P resulting in the complementary anions $[dT5P - T]^-$ and $[T - H]^-$. In deprotonated thymidine the glycosidic bond cleavage was ascribed to initial deprotonation at the sugar. However, due to the presence of the phosphate group in dT5P the fragmentation pathway is fundamentally different. Due to the differences in acidity between the sugar hydroxyl groups and the phosphoric acid a proton transfer from the sugar to the phosphate is unlikely. A nucleophilic attack from the phosphate to the 4′C of the sugar ring then leads to the formation of a cyclic phosphate and a sugar cross-ring cleavage that is followed by the elimination of the deprotonated nucleobase $[T - H]^-$ (Fig. 5d). A subsequent proton transfer from the phosphate group results in the fragment anion $[dT5 - T]^-$. Additional water elimination leads to $[dT5P - T - H_2O]^-$. Also from dT5P the phosphate ions $H_2PO_4^-$ and PO_3^- are observed, but with reversed intensity ratio compared to the sugarphosphates. The low intensity of the $H_2PO_4^-$ ion can be explained by the establishment of an intramolecular hydrogen bond between 3NH of the thymine unit and the phosphate oxygen. This reduces the probability that a suitable conformation necessary for phosphate ester pyrolysis (and $H_2PO_4^-$ formation) is adopted, and facilitates an elimination of the PO_3^- ion. On the other hand a proton transfer from 3NH to the phosphate can take place that initiates the elimination of HNCO from the thymine ring. Due to the comparably high acidity of phosphoric acid this reaction leads to formation of $[dT5P - HNCO]^-$ with the negative charge located on the phosphate group. In dT5P a sugar cross-ring cleavage is completely blocked indicating that the susceptibility of the sugar unit reported previously is not preserved in nucleotides.

We complete our comparative study with the hexameric thymidine oligomer. The metastable fragmentation mass spectrum of the deprotonated dT_6 oligomer is shown in Fig. 6. The dominant fragmentation pathway is a cleavage of the backbone at different positions of the hexamer. The most prominent cleavage occurs at the 5′C—O bonds that can also result in additional water loss. Furthermore, P—3′O and 3′C—O bond cleavages are observed. 3′C—O cleavage is always accompanied by a loss of the thymine nucleobase, i.e., glycosidic bond cleavage. The prevailing fragmentation pathway in the thymidine oligomer is the phosphodiester bond

cleavage and the glycosidic bond cleavage. Neither sugar cross-ring cleavage nor nucleobase ring cleavage is observed from deprotonated dT_6.

4. Conclusions

The metastable decay of the deprotonated hexameric oligonucleotide dT_6 is characterized by phosphoester and N-glycosidic bond cleavage. These fragmentation reactions correspond to the main DNA damage pathways induced by ionizing radiation, namely nucleobase loss and DNA strand breaks. In thymidine 5′-monophosphate these channels also dominate but also nucleobase ring cleavage is observed, corresponding to nucleobase lesions in DNA. In thymidine, the nucleobase cleavage dominates over the glycosidic bond rupture but also sugar cross-ring cleavage is observed, though to a lesser extent. Similarly the phosphate ester bond rupture dominates in ribose 5-monophosphate, as is the case for thymidine 5′-monophosphate and dT_6.

In isolated D-ribose deprotonation predominantly proceeds from the anomeric hydroxyl group and leads to sugar cross-ring cleavage. The most pronounced cross-ring cleavage observed from the isolated sugar is also observed in the sugar 5-monophosphates and in thymidine, although the anomeric hydroxyl group is replaced by the N-glycosidic bond in the latter. However, sugar cross-ring cleavage is already weak in ribose 5-monophosphate and thymidine.

The initial deprotonation site in all investigated molecules determines the specific reaction pathway. Deprotonation of thymine at the 1N site does not lead to further fragmentation, but deprotonation at the 3N site results in NCO^- formation. This fragmentation channel is preserved in thymidine and in thymidine 5′-phosphate (resulting in neutral HNCO loss). In thymidine 5′-monophosphate this fragmentation is most likely initiated by proton transfer to the phosphate.

Acknowledgments

We acknowledge financial support from the Icelandic Centre for Research (RANNIS) and the University of Iceland Research Fund. IB acknowledges support for a visit to Reykjavik by the COST action P9 (Radiation Damage in Biomolecular Systems, RADAM) and by the European Science Foundation (ESF) program: Electron induced processes at the molecular level (EIPAM). HDF acknowledges a PhD grant from the Eimskip University Fund (EUF).

References

[1] L. Sanche, Low energy electron-driven damage in biomolecules, Eur. Phys. J. D 35 (2005) 367.
[2] J. Simons, How do low-energy (0.1–2 eV) electrons cause DNA-strand breaks? Acc. Chem. Res. 39 (2006) 772.
[3] I. Baccarelli, I. Bald, F.A. Gianturco, E. Illenberger, J. Kopyra, Electron-induced damage of DNA and its components: experiments and theoretical models, Phys. Rep. 508 (2011) 1.
[4] I. Bald, J. Langer, P. Tegeder, O. Ingolfsson, From isolated molecules through clusters and condensates to the building blocks of life A short tribute to Prof. Eugen Illenberger's work in the field of negative ion chemistry, Int. J. Mass Spectrom. 277 (2008) 4.
[5] H. Abdoul-Carime, S. Gohlke, E. Illenberger, Site-specific dissociation of DNA bases by slow electrons at early stages of irradiation, Phys. Rev. Lett. 92 (2004) 168103.
[6] I. Bald, J. Kopyra, E. Illenberger, Selective excision of C5 from D-ribose in the gas phase by low-energy electrons (0–1 eV): implications for the mechanism of DNA damage, Angew. Chem. Int. Ed. 45 (2006) 4851.
[7] I. Baccarelli, F.A. Gianturco, A. Grandi, N. Sanna, R.R. Lucchese, I. Bald, J. Kopyra, E. Illenberger, Selective bond breaking in D-D-ribose by gas-phase electron attachment around 8 eV, J. Am. Chem. Soc. 129 (2007) 6269.
[8] I. Bald, I. Dabkowska, E. Illenberger, Probing biomolecules by laser-induced acoustic desorption: electrons at near zero electron volts trigger sugar–phosphate cleavage, Angew. Chem. Int. Ed. 47 (2008) 8518.
[9] C. Konig, J. Kopyra, I. Bald, E. Illenberger, Dissociative electron attachment to phosphoric acid esters: the direct mechanism for single strand breaks in DNA, Phys. Rev. Lett. 97 (2006) 018105.
[10] S. Ptasinska, S. Denifl, S. Gohlke, P. Scheier, E. Illenberger, T.D. Maerk, Decomposition of thymidine by low-energy electrons: implications for the molecular mechanisms of single-strand breaks in DNA, Angew. Chem. Int. Ed. 45 (2006) 1893.
[11] S. Ptasinska, S. Denifl, P. Scheier, E. Illenberger, T.D. Maerk, Bond- and site-selective loss of H atoms from nucleobases by very-low-energy electrons (<3 eV), Angew. Chem. Int. Ed. 44 (2005) 6941.
[12] S. Denifl, F. Zappa, A. Mauracher, F.F. da Silva, A. Bacher, O. Echt, T.D. Mark, D.K. Bohme, P. Scheier, ChemPhysChem 9 (2008) 1387.
[13] H.D. Flosadottir, S. Denifl, F. Zappa, N. Wendt, A. Mauracher, A. Bacher, H. Jonsson, T.D. Maerk, P. Scheier, O. Ingolfsson, Combined experimental and theoretical study on the nature and the metastable decay pathways of the amino acid ion fragment [M−H], Angew. Chem. Int. Ed. 46 (2007) 8057.
[14] M. Stano, H.D. Flosadottir, O. Ingolfsson, Effective quenching of fragment formation in negative ion oligonucleotide matrix-assisted laser desorption/ionization mass spectrometry through sodium adduct formation, Rapid Commun. Mass Spec. 20 (2006) 3498.
[15] S. Breeger, M. von Meltzer, U. Hennecke, T. Carell, Investigation of the pathways of excess electron transfer in DNA with flavin-donor and oxetane-acceptor modified DNA hairpins, Chem. Eur. J. 12 (2006) 6469.
[16] A.M. Lamsabhi, M. Alcami, O. Mo, M. Yanez, J. Tortajada, J.Y. Salpin, Unimolecular reactivity of uracil-Cu2(+) complexes in the gas phase, ChemPhysChem 8 (2007) 181.
[17] CRC Handbook of Chemistry and Physics, CRC Press, 2002.
[18] E.C.M. Chen, C. Herder, E.S. Chen, The experimental and theoretical gas phase acidities of adenine, guanine, cytosine, uracil, thymine and halouracils, J. Mol. Struct. 798 (2006) 126.
[19] I. Bald, H.D. Flosadottir, J. Kopyra, E. Illenberger, O. Ingolfsson, Fragmentation of deprotonated D-ribose and D-fructose in MALDI—comparison with dissociative electron attachment, Int. J. Mass Spectrom. 280 (2009) 190.
[20] H.D. Flosadottir, H. Jonsson, S.T. Sigurdsson, O. Ingolfsson, Experimental and theoretical study of the metastable decay of negatively charged nucleosides in the gas phase, Phys. Chem. Chem. Phys. 13 (2011) 15283.
[21] H.D. Flosadottir, I. Bald, O. Ingolfsson, Fast and metastable fragmentation of deprotonated D-fructose—a combined experimental and computational study, Int. J. Mass Spectrom. 305 (2011) 50.
[22] R.A. Morris, W.B. Knighton, A.A. Viggiano, B.C. Hoffman, H.F. Schaefer, The gas-phase acidity of H_3PO_4, J. Chem. Phys. 106 (1997) 3545.
[23] J.-Y. Salpin, J. Tortajada, Gas-phase acidity of D-glucose. A density functional theory study, J. Mass Spectrom. 39 (2004) 930.